Journal of Water Resource and Protection, 2026, 18(3), 186-207
https://www.scirp.org/journal/jwarp
ISSN Online: 1945-3108
ISSN Print: 1945-3094

# Controlling Factors of Water Chemistry along the Zacate Creek, an Urban Tributary of the Rio Grande in Texas

**Maya Prakash Bhatt[1*], Ganesh Bahadur Malla[2], Pranaad Kolwadkar[1], Elizabeth Tran[1], Seema Bhatt[1], Alfred Addo-Mensah[1*]**

[1]Department of Biology and Chemistry, Texas A&M International University, Laredo, TX, USA
[2]Department of Mathematics, Computer, Geology and Physics, University of Cincinnati-Clermont, Batavia, OH, USA
Email: *maya.bhatt@tamiu.edu, *alfred.addo-mensah@tamiu.edu

**How to cite this paper:** Bhatt, M.P., Malla, G.B., Kolwadkar, P., Tran, E., Bhatt, S. and Addo-Mensah, A. (2026) Controlling Factors of Water Chemistry along the Zacate Creek, an Urban Tributary of the Rio Grande in Texas. *Journal of Water Resource and Protection*, **18**, 186-207.
https://doi.org/10.4236/jwarp.2026.183011

**Received:** January 14, 2026
**Accepted:** March 6, 2026
**Published:** March 9, 2026



## Abstract

Stream water samples were collected along Zacate Creek, a small urban tributary of the Rio Grande in Laredo, South Texas, to investigate the spatiotemporal variability and controlling factors of water quality across the drainage network. The hydrochemical composition was dominated by sodium among cations and sulfate among anions, with major ions occurring in the order $Na^+ \gg Ca^{2+} > Mg^{2+} \approx K^+$ and $SO_4^{2-} \gg Cl^- > HCO_3^- \gg NO_3^- \gg PO_4^{3-}$. Marine aerosols were identified as a significant source of sodium (49%) and magnesium (44%), while contributing only minor proportions of sulfate, calcium, and potassium. In addition to atmospheric inputs, chemical weathering primarily of carbonate and aluminosilicate minerals plays a key role in regulating the overall water chemistry of Zacate Creek. The results indicate strong seasonal controls on water chemistry, whereas spatial variations along the drainage network were comparatively minor. Magnesium, nitrate, bicarbonate, hardness, and alkalinity displayed pronounced winter-summer differences, reflecting higher ionic strength and nutrient concentrations during winter conditions. Bivariate correlation and regression analyses showed strong linear relationships ($|r| \geq 0.85$) among major ions, electrical conductivity, total dissolved solids, hardness, sodium adsorption ratio, and boron, indicating that dissolved ionic constituents exert dominant control over creek hydrochemistry. Multivariate modeling further confirmed that water chemistry is governed by integrated ionic, carbonate, and salinity-driven processes on selected parameters and exceptionally high predictive performance ($R^2 \approx 1.0$). Sodium and magnesium maintained relatively stable sea-salt contributions throughout the year, while sea-salt-derived sulfate exhibited notable winter enrichment, highlighting the influence of temperature and flow-dependent processes. Over-

all, the findings demonstrate a tightly coupled hydrogeochemical framework controlled by chemical weathering, marine aerosol inputs, and seasonal hydrology under variable climatic conditions.

## Keywords

Major Ions, Sea-Salt Correction, Weathered Contribution, Multivariate Hydrochemical Modeling, Zacate Creek, Rio Grande

## 1. Introduction

Arid and semi-arid regions worldwide including North Africa, Middle East, Central Asia, Australia, the southwestern United States, and large areas of Sub-Saharan Africa faces sever challenges related to both water quantity and quality because freshwater resources are naturally limited, highly variable, and increasingly stressed climate driven drought, high evaporative demand and increasing water use demand [1]-[5]. Basin-scale water-quality monitoring of any landscape is essential for protecting public health, conserving ecosystems, meeting regulatory requirements, safeguarding source waters, and improving treatment efficiency [6] [7]. Small urban streams in arid and semi-arid regions often exhibit pronounced spatiotemporal variability in water chemistry, yet they remain understudied. In South Texas, many tributaries of the Rio Grande, including Zacate Creek in Laredo, experience highly variable flow regimes driven by seasonal rainfall, prolonged dry periods, and increasing urban development. These factors create dynamic hydrologic and geochemical conditions that can change markedly over short spatial and temporal scales [8]-[11]. Zacate Creek drains into a rapidly urbanizing catchment where natural hydrological processes are increasingly modified by stormwater infrastructure, channel alteration, and impervious surfaces along the drainage network within Laredo. During dry periods, surface flow is often minimal or limited to isolated pools sustained by shallow groundwater inputs in the region. In contrast, rainfall events generate short-lived runoff (flash flood) that mobilizes accumulated solutes from soils, road surfaces, and stream sediments hence the natural chemistry of the stream is altered. As a result, stream chemistry can shift rapidly between groundwater-dominated and runoff-dominated conditions, making Zacate Creek an ideal system for examining spatiotemporal controls on water chemistry [12] [13]. Studies in the Laredo area show that small urban tributaries can be important sources of chemicals entering the Rio Grande. For example, Manadas Creek, located near Zacate Creek, has been found to contain high levels of trace metals such as antimony, arsenic, and nickel, which are linked to past industrial activities and urban runoff [14]. The Zacate Creek watershed faces similar pressures from urban activities. While the creek contributes to a smaller volume of water than the Rio Grande itself, its chemical makeup, especially during stormflow, can influence downstream conditions by raising salinity, conductivity,

nutrient concentrations, and suspended sediment loads.

In semi-arid environments, the chemical composition of surface waters is commonly influenced by a combination of carbonate weathering, evaporative concentration, and anthropogenic inputs and similar type of results in regulating water chemistry from geochemical processes including evaporite weathering and anthropogenic activities recently documented by Tao *et al.* (2025) [15] in a semi-arid watershed. Classic studies have shown that major-ion chemistry in rivers reflects the balance among rock-water interactions, atmospheric inputs, and evaporation-crystallization processes [16] [17]. In South Texas, carbonate-rich soils, caliche layers, and sedimentary bedrock contribute calcium, magnesium, and bicarbonate to surface waters, while high temperatures and evaporation further concentrate dissolved ions [1]. Urbanization adds an additional layer of complexity, as road runoff, wastewater infrastructure, and altered flow paths introduce sodium, chloride, sulfate, and nutrients, often resulting in elevated salinity and shifts in hydrochemical facies [18]-[20]. However, the relative contributions of natural versus anthropogenic solute sources in small urban streams of South Texas remain poorly constrained, particularly across seasonal and hydrologic conditions.

The objective of this study was to assess the controlling factors of water chemistry along Zacate Creek to provide critical insights into how hydrology, geology, climate, and urban land use interact to shape stream geochemistry. By examining longitudinal patterns along the creek and seasonal contrasts between dry and wet periods, this study aims to distinguish background geochemical signatures from event-driven and anthropogenic influences. Such information is essential for establishing baseline conditions, improving urban watershed management, and understanding the response of semi-arid stream and connected lake-pond ecosystems to ongoing environmental change [21]-[25]. Univariate, bivariate, and multivariate regression analyses were employed to evaluate the biogeochemical controls on water quality along Zacate Creek across seasonal cycles. The findings of this study provide a scientific basis for sustainable watershed and water-quality management strategies in the region and in comparable urban watersheds worldwide.

## 2. Study Area

Zacate Creek, an urban stream located in Laredo, Southern Texas, is a tributary to Rio Grande, a major river system in the US. Zacate Creek flows through the urban center of Laredo and finally mixes with the Rio Grande near the bridge at the international border between US and Mexico (**Figure 1**). Rio Grande originates in south-central Colorado and flows through the arid and semi-arid areas all the way down to the Gulf of America-Mexico and has a drainage area of 472,000 $km^2$ [26]. The length of Rio Grande is 3051 km which is considered the fourth largest river system in the United States and North America [26]. Rio Grande is a vital waterway for communities along the USA-Mexico border and river provides drinking water to over six million people, supports irrigation and industry, and sustains

valuable aquatic and riparian ecosystems [27] [28]. The Rio Grande receives water from numerous smaller tributaries that drain urban, agricultural, and industrial landscapes and even though these tributaries often carry only small amounts of water, they can have an outsized impact on downstream water quality, particularly during storm events [27].

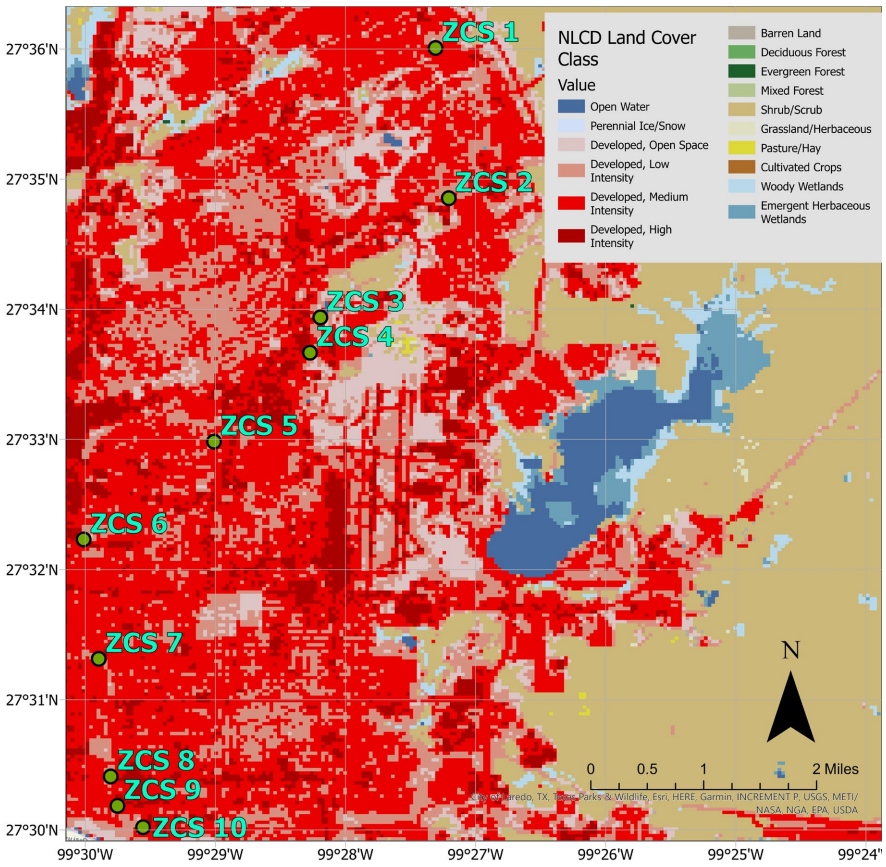


**Figure 1.** Sampling locations of Zacate Creek with land cover classes within Laredo, Southern Texas.

Biogeochemical processes completely altered downstream sites due to human activities including land use change patterns, mining activities, urban drainage, agricultural activities, business complexes, deforestation and development activities in the region. Chemical loads are expected to increase in downstream sites due to accumulation, and such patterns have been previously reported in Manadas Creek and pond ecosystems in the same area [14] [23]-[25]. High concentrations of chemical loads can impact the ecology of the stream. The complete water quality status of the Zacate Creek and the lower Rio Grande has not been done before.

Laredo is situated at an altitude of 127.41 m asl on the Mexican border in Southern Texas with an area of about 265.7 km$^2$ with a large area surrounded by forest [25]. The Mean Annual Temperature (MAT) and Mean Annual Precipitation (MAP) in Laredo are 23.8˚C and 525.3 mm, respectively and August is the hottest month of the year with a maximum of 38.3˚C to minimum of 25.0˚C and generally

January is the coldest month in Laredo and the cold starts from the middle of December and stretches up to early February [29].

## 3. Materials and Methods

### 3.1. Sample Collection

Zacate Creek water samples were collected from ten different locations with a total of 30 samples representing three different seasons: September 2024 (fall), early March 2025 (winter), and late May 2025 (summer) (**Figure 1**). Surface runoff from urban areas enters the stream from all the sampling locations along the drainage network. Physical parameters such as water temperature, pH, EC, DO, and TDS were measured at the time of sampling in the field. Samples were taken in 250 mL acid-washed polyethylene bottles, and refrigerated at the laboratory of Texas A&M International University (TAMIU) and samples were packed in ice and sent to soil and water testing lab of the Texas A&M University in college station for the analysis of major base cations ($Na^+$, $K^+$, $Mg^{2+}$, $Ca^{2+}$), major anions ($Cl^-$, $NO_3^-$, $SO_4^{2-}$, $HCO_3^-$, $PO_4^{3-}$), hardness, alkalinity, sodium adsorption ratio (SAR) and boron. Carbonate ion was not detected in any location.

### 3.2. Analytical Methods

Water temperature, pH, EC, DO, and TDS were measured at the time of sampling by using handheld meter, Thermo Scientific™ Orion Star™ A329. Chloride was determined by ion chromatography using US EPA method 300.0 [30]. $NO_3$-N is measured by reduction of nitrite ($NO_2$-N) to nitrate by using cadmium column followed by spectrophotometric measurement [31]. Sulfate was calculated from total sulfur [31]. Ammonium ($NH_4$-N) was measured by spectrophotometric measurement [31]. Fluorine was determined directly using fluoride selective electrode (APHA 1989). Samples were filtered through a 0.45 µm polycarbonate filter for Na, K, Mg, Ca, S, P, Fe, Zn, Cu, Mn, As, Ba, Cd, Cr, Ni, and Pb analysis by using Inductively Coupled Plasma Emission Spectroscopy (ICP-ES) [31]. Trace element concentrations were found to be too low and were not used for modeling or further analysis. Carbonate and bicarbonate are determined by titration using sulfuric acid, alkalinity is calculated from carbonate and bicarbonate concentrations and hardness is calculated from Ca and Mg concentrations [31]. TDS is calculated by summing the cations and anions. Sodium Absorption Ratios (SAR) are calculated from sodium, calcium and magnesium concentrations. Charge balance is calculated by dividing the sum of cations by the sum of anions and it is less than 5% for all samples [31].

## 4. Results

### 4.1. Seasonal Variation in Water Temperature at Zacate Creek

Physical and chemical parameters of Zacate Creek, located in Laredo, Southern Texas, were monitored from September 2024 to May 2025 to capture seasonal variations across fall, spring, and summer. **Table 1** and **Figure 2** summarize sea-

sonal water temperature patterns in Zacate Creek based on 30 observations. Average temperatures vary by season, with the highest mean occurring in summer (31.8˚C) and the lowest in winter (25.6˚C), while fall shows intermediate values (26.6˚C). Summer temperatures are consistently warmer, with a relatively narrow 95% confidence interval (29.8˚C - 33.9˚C), indicating stable conditions. Winter exhibits the greatest variability, reflected in the largest standard deviation (3.9˚C) and the widest confidence interval (22.8˚C - 28.4˚C). Overall, the combined data yielded an average water temperature of 28.0˚C, with observed values ranging from 21.0˚C to 35.6˚C, highlighting clear seasonal differences in thermal conditions along the Zacate Creek.

**Table 1.** Seasonal variation in water temperature at Zacate Creek.

| Season | n | Average (˚C) | Standard Deviation | 95% Confidence Interval for Mean | | Min | Max |
|---|---|---|---|---|---|---|---|
| | | | | Lower Bound | Upper Bound | | |
| Fall | 10 | 26.6 | 1.7 | 25.5 | 27.8 | 24.9 | 30.0 |
| Winter | 10 | 25.6 | 3.9 | 22.8 | 28.4 | 21.0 | 32.1 |
| Summer | 10 | 31.8 | 2.8 | 29.8 | 33.9 | 29.1 | 35.6 |
| Total | 30 | 28.0 | 3.9 | 26.5 | 29.5 | 21.0 | 35.6 |

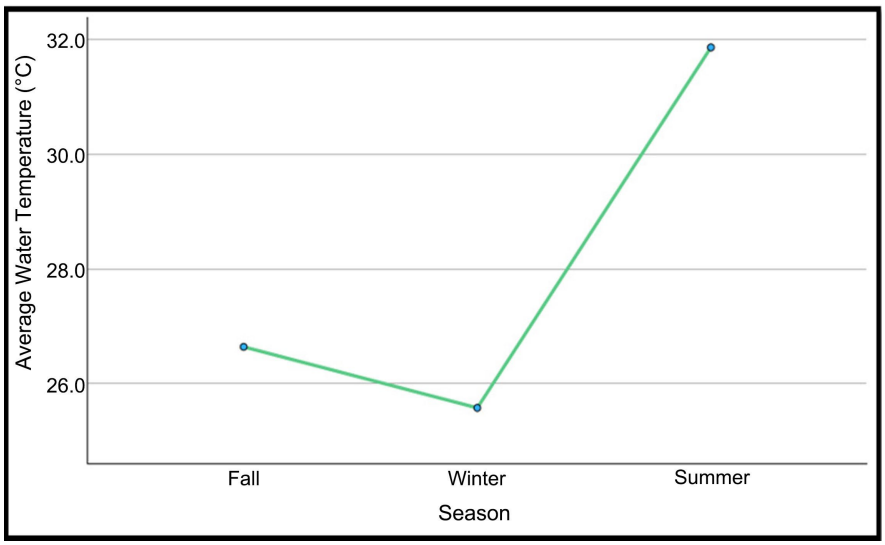


**Figure 2.** Average water temperature plot.

## 4.2. Seasonal Variation and Statistical Significance of Water Quality Parameters

To examine seasonal variation in the physical and chemical parameters of Zacate Creek, an Analysis of Variance (ANOVA) test was performed to evaluate the null hypothesis that seasonal temperature differences exert no significant influence on the measured parameters. The first column of **Table 2** lists all measured parameters under study with their respective units, while columns 2 - 4 present the seasonal mean ± standard deviation for fall, winter, and summer, respectively. Col-

umns 5 - 7 provide the corresponding Fisher's F-statistic, degrees of freedom (DF), and p-values. Statistically significant results, where the null hypothesis was rejected, are indicated by palm branch (🌿) in the final column.

**Table 2.** Seasonal ANOVA results for physical and chemical parameters of Zacate Creek.

| Measured Parameters | Fall Mean ± SD | Winter Mean ± SD | Summer Mean ± SD | F | DF | p-value |
|---|---|---|---|---|---|---|
| pH | 8.27 ± 0.61 | 8.18 ± 0.68 | 8.38 ± 0.44 | 0.299 | (2, 27) | 0.744 |
| DO (mg/L) | 7.02 ± 3.44 | 9.35 ± 2.58 | 9.01 ± 2.59 | 1.893 | (2, 27) | 0.170 |
| EC (µS/cm) | 3954 ± 2016 | 4523 ± 1837 | 3129 ± 1250 | 1.637 | (2, 27) | 0.213 |
| TDS (mg/L) | 2654 ± 1415 | 3691 ± 1588 | 2362 ± 965 | 2.684 | (2, 27) | 0.086 |
| $Ca^{2+}$ (mg/L) | 211.4 ± 86.5 | 276.4 ± 96.6 | 183.2 ± 62.1 | 3.312 | (2, 27) | 0.052 |
| $Mg^{2+}$ (mg/L) | 72.9 ± 39.8 | 109.7 ± 49.4 | 59.1 ± 28.6 | 4.226 | (2, 27) | **0.025**🌿 |
| $Na^{+}$ (mg/L) | 560.4 ± 318.7 | 797.6 ± 391.9 | 236.8 ± 74.9 | 2.464 | (2, 27) | 0.104 |
| $K^{+}$ (mg/L) | 7.3 ± 2.3 | 7 ± 4.3 | 7.4 ± 2.3 | 0.045 | (2, 27) | 0.956 |
| $Cl^{-}$ (mg/L) | 483.6 ± 275.4 | 713.1 ± 336.2 | 402.3 ± 198.7 | 3.412 | (2, 27) | 0.058 |
| $NO_3^-$ (mg/L) | 0.36 ± 0.66 | 19.05 ± 9.36 | 0.47 ± 0.74 | 39.157 | (2, 27) | **< 0.001**🌿 |
| $SO_4^{2-}$ (mg/L) | 1164.5 ± 725.9 | 1582.7 ± 722.0 | 1097.9 ± 477.8 | 1.622 | (2, 27) | 0.216 |
| $PO_4^{3-}$ (mg/L) | 0.011 ± 0.003 | 0.081 ± 0.138 | 0.037 ± 0.025 | 1.884 | (2, 27) | 0.171 |
| $HCO_3^-$ (mg/L) | 151.5 ± 46.7 | 185.4 ± 33.3 | 115.3 ± 42.4 | 7.230 | (2, 27) | **0.003**🌿 |
| Hardness (mg/L) | 828.2 ± 364.7 | 1142.1 ± 428.3 | 700.2 ± 247.9 | 4.103 | (2, 27) | **0.027**🌿 |
| Alk (mg/L) | 124.5 ± 38.5 | 151.9 ± 27.4 | 97 ± 40.1 | 5.866 | (2, 27) | **0.007**🌿 |
| SAR | 8.04 ± 3.18 | 9.71 ± 4.12 | 7.85 ± 2.97 | 0.873 | (2, 27) | 0.428 |
| B (mg/L) | 2.18 ± 1.25 | 2.67 ± 1.33 | 1.62 ± 0.77 | 2.096 | (2, 27) | 0.142 |
| CB (%) | 102.6 ± 6.7 | 99.6 ± 1.8 | 98.2 ± 2.7 | 2.726 | (2, 27) | 0.083 |

Note: 🌿 = Statistically significant.

The one-way ANOVA results indicate that most physical and chemical parameters of Zacate Creek do not show statistically significant seasonal differences ($p > 0.05$), including pH, Dissolved Oxygen (DO), Electrical Conductivity (EC), Total Dissolved Solids (TDS), $Na^+$, $K^+$, $Ca^{2+}$, $Cl^-$, $SO_4^{2-}$, $PO_4^{3-}$, SAR, Boron (B), and Charge Balance (CB). In contrast, five parameters exhibit significant seasonal variation: $Mg^{2+}$ ($p = 0.025$), $NO_3^-$ ($p < 0.001$), $HCO_3^-$ ($p = 0.003$), hardness ($p = 0.027$), and alkalinity ($p = 0.007$). Several other parameters (e.g., $Ca^{2+}$, $Cl^-$, TDS, CB) show near-significant trends ($0.05 < p < 0.10$) but do not meet the conventional significance threshold.

### Interpretation of Significant Parameters with Bonferroni Results

Bonferroni post hoc comparisons clarify that the observed seasonal effects are primarily driven by winter-summer contrasts. Magnesium concentrations are signif-

icantly higher in winter than in summer, suggesting enhanced mineral input or reduced dilution during colder months. Nitrate shows a pronounced winter peak, with fall and summer not differing significantly, indicating seasonally elevated nutrient loading or reduced biological uptake in winter. Similarly, $HCO_3^-$, hardness, and alkalinity are all significantly greater in winter compared to summer, reflecting increased carbonate weathering influence, reduced streamflow dilution, or groundwater contributions during winter conditions. Collectively, these results highlight winter as the season with elevated ionic strength and nutrient levels, while summer conditions reflect comparatively diluted or biologically moderated water chemistry in Zacate Creek.

### 4.3. Bivariate Analysis of Highly Correlated Variable Pairs (|r| ≥ 0.85) in Zacate Creek Water

To avoid redundancy and improve clarity in presenting the 18 × 18 bivariate correlation and regression analyses of Zacate Creek water, this study focuses exclusively on highly correlated variable pairs**.** Accordingly, only pairs with an absolute Pearson correlation coefficient of |r| ≥ 0.85 were selected for further examination. Table 3 summarizes the 41 highly correlated pairs**,** reporting their corresponding Pearson correlation coefficients and their predictive models that highlight the dominant interrelationships governing the hydrochemical behavior along Zacate Creek.

Table 3. Correlation and regression analyses of highly correlated variable pairs (|r| ≥ 0.85).

| Model Number | Dependent Variable (DV) | Predictor | \|r\| | Predictive model | | $R^2$-value | p-value |
|---|---|---|---|---|---|---|---|
| | | | | DV-Intercept | Slope | | |
| 1 | EC | TDS | 0.978 | **342.735** | **1.215** | **0.956** | **<0.001** |
| 2 | EC | Calcium | 0.877 | **−14.685** | **17.361** | **0.769** | **<0.001** |
| 3 | EC | Magnesium | 0.937 | **864.052** | **37.289** | **0.878** | **<0.001** |
| 4 | EC | Sodium | 0.971 | **730.178** | **5.086** | **0.943** | **<0.001** |
| 5 | EC | Chloride | 0.965 | **813.815** | **5.731** | **0.931** | **<0.001** |
| 6 | EC | Sulfate | 0.979 | **533.543** | **2.602** | **0.959** | **<0.001** |
| 7 | EC | Hardness | 0.940 | **82.993** | **4.252** | **0.883** | **<0.001** |
| 8 | EC | SAR | 0.940 | **−251.987** | **482.846** | **0.884** | **<0.001** |
| 9 | EC | Boron | 0.985 | **710.194** | **1462.3112** | **0.970** | **<0.001** |
| 10 | TDS | Calcium | 0.907 | **−330.118** | **14.453** | **0.823** | **<0.001** |
| 11 | TDS | Magnesium | 0.966 | **408.859** | **30.950** | **0.934** | **<0.001** |
| 12 | TDS | Sodium | 0.992 | **322.825** | **4.180** | **0.984** | **<0.001** |
| 13 | TDS | Chloride | 0.990 | **379.933** | **4.733** | **0.980** | **<0.001** |
| 14 | TDS | Sulfate | 0.992 | **184.263** | **2.121** | **0.984** | **<0.001** |
| 15 | TDS | Hardness | 0.971 | **−244.444** | **3.535** | **0.942** | **<0.001** |
| 16 | TDS | SAR | 0.942 | **−421.286** | **389.498** | **0.888** | **<0.001** |

**Continued**

| | | | | | | | |
|---|---|---|---|---|---|---|---|
| 17 | TDS | Boron | 0.980 | **372.185** | **1171.592** | **0.961** | **<0.001** |
| 18 | Calcium | Chloride | 0.902 | **79.361** | **0.271** | **0.814** | **<0.001** |
| 19 | Calcium | Hardness | 0.969 | **26.430** | **0.222** | **0.939** | **<0.001** |
| 20 | Calcium | Boron | 0.895 | **78.666** | **67.141** | **0.801** | **<0.001** |
| 21 | Magnesium | Sodium | 0.964 | **2.269** | **0.127** | **0.930** | **<0.001** |
| 22 | Magnesium | Chloride | 0.967 | **3.638** | **0.144** | **0.935** | **<0.001** |
| 23 | Magnesium | Sulfate | 0.940 | **0.099** | **0.063** | **0.884** | **<0.001** |
| 24 | Magnesium | Hardness | 0.954 | **−15.995** | **0.108** | **0.910** | **<0.001** |
| 25 | Magnesium | SAR | 0.899 | **−18.459** | **11.605** | **0.809** | **<0.001** |
| 26 | Magnesium | Boron | 0.956 | **3.523** | **35.674** | **0.914** | **<0.001** |
| 27 | Sodium | Chloride | 0.985 | **21.548** | **1.117** | **0.970** | **<0.001** |
| 28 | Sodium | Sulfate | 0.983 | **−22.258** | **0.499** | **0.966** | **<0.001** |
| 29 | Sodium | Hardness | 0.941 | **−106.712** | **0.813** | **0.885** | **<0.001** |
| 30 | Sodium | SAR | 0.971 | **−195.158** | **95.183** | **0.942** | **<0.001** |
| 31 | Sodium | Boron | 0.976 | **19.540** | **276.676** | **0.952** | **<0.001** |
| 32 | Chloride | Sulfate | 0.970 | **−22.950** | **0.434** | **0.940** | **<0.001** |
| 34 | Chloride | Hardness | 0.968 | **−123.517** | **0.738** | **0.937** | **<0.001** |
| 35 | Chloride | SAR | 0.928 | **−151.929** | **80.265** | **0.862** | **<0.001** |
| 36 | Chloride | Boron | 0.973 | **7.901** | **243.14** | **0.946** | **<0.001** |
| 37 | Sulfate | Hardness | 0.946 | **−153.539** | **1.612** | **0.896** | **<0.001** |
| 38 | Sulfate | Boron | 0.969 | **112.183** | **541.526** | **0.938** | **<0.001** |
| **39** | Hardness | Boron | 0.959 | **210.933** | **314.509** | **0.919** | **<0.001** |
| 40 | SAR | Boron | 0.932 | **2.710** | **2.696** | **0.870** | **<0.001** |
| 41 | Bicarbonate | Alkalinity | 0.995 | **3.366** | **1.184** | **0.989** | **<0.001** |

**NB:** EC = Electrical Conductivity; TDS = Total Dissolved Solids; SAR = Sodium Adsorption Ratio.

**Model Illustration and Interpretation:** To aid readers in understanding the representation and interpretation of the regression models summarized in Table 3, Model 1 is presented here as an illustrative example. This model describes the linear relationship between Electrical Conductivity (EC) and Total Dissolved Solids (TDS) in Zacate Creek water.

The fitted regression equation is:

$$\widehat{\mathrm{EC}} = 342.735 + 1.215(\mathrm{TDS})$$

with a coefficient of determination ($R^2 = 0.956$).

The high $R^2$ value indicates that 95.6% of the total variability in EC is explained solely by TDS, while only 4.4% of the variability remains unexplained, reflecting an exceptionally strong linear association between these two parameters which obviously we expect.

The slope (1.215) represents the rate of change in EC with respect to TDS. Specifically, for every one-unit increase in TDS, EC increases on average by 1.215 units, indicating that EC responds strongly and proportionally to changes in dissolved solids. This relationship underscores the dominant role of dissolved ionic constituents in controlling the electrical conductivity of Zacate Creek water.

Furthermore, the p-value (<0.001) associated with the regression slope indicates that the relationship between EC and TDS is highly statistically significant. Consequently, the null hypothesis that EC and TDS are independent is rejected, confirming a strong and meaningful linear dependence between the two variables, which is obvious for these two parameters. Figure 3 represents the graphics of the equation.

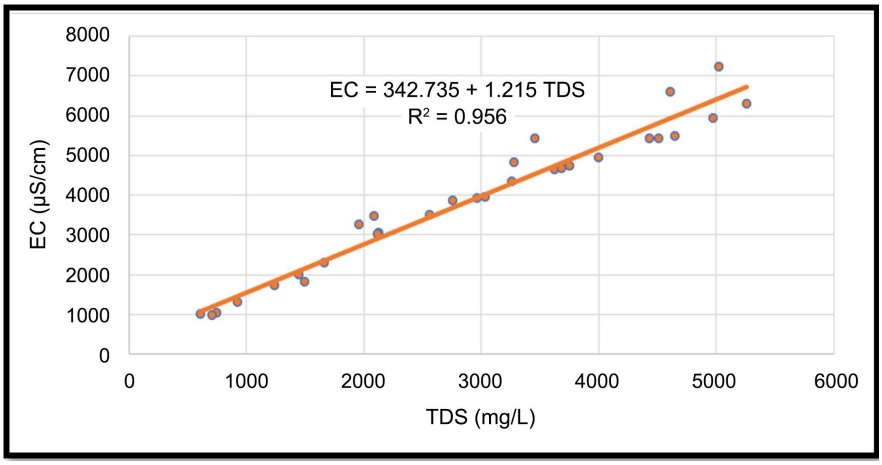


Figure 3. Bivariate relationship between EC and TDS.

## 4.4. Multivariate Modeling of Water Quality Parameters

Table 4 summarizes the multivariable regression models describing the dynamics of Zacate Creek water chemistry. Each model represents a key physicochemical parameter as a function of selected hydrochemical and ionic predictors, highlighting the interdependence among major ions, nutrients, and water quality indicators. The relatively high coefficients of determination ($R^2$ = 0.707 - 1.000) indicate strong explanatory power, reflecting systematic geochemical controls and mixing processes governing water chemistry in the creek.

The Backward Regression Method was employed for this analysis to systematically refine each model by removing statistically insignificant predictors, thereby enhancing model parsimony and interpretability. This approach minimizes multicollinearity among variables and ensures that only the most influential parameters are retained, providing a robust representation of the seasonal relationships governing the chemical composition of Zacate Creek.

**Interpretation of Multivariate Models:** Table 4 presents a comprehensive suite of 16 multivariate regression models, developed to predict the behavior of major physical and chemical parameters in Zacate Creek. In total, the analysis produced 16 predictive equations for parameters showing minimal seasonal de-

pendence. Collectively, these models comprise over 119 partial regression coefficients, each quantifying the partial influence of one variable on another while holding other predictors constant. Such coefficients encode detailed information on the interconnected chemical dynamics of the pond, offering a robust empirical framework for understanding system-wide geochemical interactions.

**Table 4.** Spatial-multivariate models of water quality parameters in Zacate Creek.

| Model Number | Parameter | Predictive Model | $R^2$ value |
|---|---|---|---|
| 1 | pH | $\widehat{\mathrm{pH}} = 8.049 + 0.092\,\mathrm{DO} + 0.001\,\mathrm{EC} - 0.021\,\mathrm{Mg^{2+}} - 0.003\,\mathrm{Ca^{2+}} - 0.002\,\mathrm{Na^{+}} - 0.004\,\mathrm{HCO_3^{-}}$ | 0.788 |
| 2 | DO | $\widehat{\mathrm{DO}} = -27.502 - 0.005\,\mathrm{EC} + 0.024\,\mathrm{Ca^{2+}} + 0.144\,\mathrm{Mg^{2+}} - 0.016\,\mathrm{Na^{+}} - 0.194\,\mathrm{NO_3^{-}} - 4.119\,\mathrm{B} + 4.154\,\mathrm{pH}$ | 0.707 |
| 3 | EC | $\widehat{\mathrm{EC}} = -1905.922 + 9.354\,\mathrm{Mg^{2+}} - 19.245\,\mathrm{NO_3^{-}} + 0.918\,\mathrm{SO_4^{2-}} + 735.341\,\mathrm{B} + 325.845\,\mathrm{pH} - 37.023\,\mathrm{DO}$ | 0.990 |
| 4 | **$Ca^{2+}$** | $\widehat{\mathrm{Ca^{2+}}} = 0.383 - 1.647\,\mathrm{Mg^{2+}} - 0.025\,\mathrm{NO_3^{-}} + 0.302\,\mathrm{Hardness} - 0.004\,\mathrm{Alk} + 0.194\,\mathrm{SAR} - 0.035\,\mathrm{DO} - 0.02\,\mathrm{EC}$ | 0.985 |
| 5 | **$Mg^{2+}$** | $\widehat{\mathrm{Mg^{2+}}} = 0.014 - 0.603\,\mathrm{Ca^{2+}} + 0.00308\,\mathrm{Na^{+}} - 0.002\,\mathrm{Cl^{-}} - 0.019\,\mathrm{NO_3^{-}} + 0.018\,\mathrm{HCO_3^{-}} + 0.243\,\mathrm{Hardness}$ | 0.992 |
| 6 | **$Na^{+}$** | $\widehat{\mathrm{Na^{+}}} = -309.576 - 0.66612\,\mathrm{Mg^{2+}} + 0.473\,\mathrm{Cl^{-}} + 1.851\,\mathrm{NO_3^{-}} + 0.250\,\mathrm{SO_4^{2-}} + 0.450\,\mathrm{Alk} + 22.397\,\mathrm{SAR} + 26.282\,\mathrm{B} + 2.427\,\mathrm{CB} - 0.678\,\mathrm{Ca^{2+}}$ | 0.999 |
| 7 | **$K^{+}$** | $\widehat{\mathrm{K^{+}}} = -21.334 - 0.109\,\mathrm{Mg^{2+}} + 0.041\,\mathrm{Cl^{-}} + 0.021\,\mathrm{SO_4^{2-}} + 28.111\,\mathrm{PO_4^{3-}} - 0.315\,\mathrm{HCO_3^{-}} + 0.435\,\mathrm{CB} - 2.125\,\mathrm{pH} - 0.052\,\mathrm{Ca^{2+}} - 0.0456\,\mathrm{Na^{+}}$ | 0.729 |
| 8 | **$Cl^{-}$** | $\widehat{\mathrm{Cl^{-}}} = 638.808 + 1.621\,\mathrm{Mg^{2+}} - 1.709\,\mathrm{NO_3^{-}} - 0.413\,\mathrm{SO_4^{2-}} - 0.859\,\mathrm{Alk} - 28.922\,\mathrm{SAR} - 5.344\,\mathrm{CB} + 1.212\,\mathrm{Ca^{2+}} + 1.495\,\mathrm{Na^{+}}$ | 0.996 |
| 9 | $NO_3^{-}$ | $\widehat{\mathrm{NO_3^{-}}} = -42.104 + 4.443\,\mathrm{pH} - 0.013\,\mathrm{EC} + 0.106\,\mathrm{Ca^{2+}} + 0.253\,\mathrm{Mg^{2+}} + 0.064\,\mathrm{Na^{+}} - 0.019\,\mathrm{SO_4^{2-}}$ | 0.883 |
| 10 | $SO_4^{2-}$ | $\widehat{\mathrm{SO_4^{2-}}} = 0.508 + 1.000\,\mathrm{DO} - 1.051\,\mathrm{Ca^{2+}} - 0.989\,\mathrm{Mg^{2+}} - 1.023\,\mathrm{Na^{+}} - 0.996\,\mathrm{K^{+}} - 0.950\,\mathrm{Cl^{-}} - 0.949\,\mathrm{NO_3^{-}}$ | 0.988 |
| 11 | $PO_4^{3-}$ | $\widehat{\mathrm{PO_4^{3-}}} = 0.631 + 0.004\,\mathrm{NO_3^{-}} + 0.008\,\mathrm{HCO_3^{-}} - 0.010\,\mathrm{CB} + 0.019\,\mathrm{K^{+}} - 0.001\,\mathrm{Cl^{-}}$ | 0.738 |
| 12 | $HCO_3^{-}$ | $\widehat{\mathrm{HCO_3^{-}}} = 1.743 + 0.997\,\mathrm{TDS} - 1.045\,\mathrm{Ca^{2+}} - 0.957\,\mathrm{Mg^{2+}} - 1.022\,\mathrm{Na^{+}} - 0.954\,\mathrm{K^{+}} - 0.953\,\mathrm{Cl^{-}} - 0.926\,\mathrm{NO_3^{-}}$ | 0.996 |
| 13 | Alkalinity | $\widehat{\mathrm{Alk}} = -2.875 + 0.845\,\mathrm{TDS} - 0.888\,\mathrm{Ca^{2+}} - 0.882\,\mathrm{Mg^{2+}} - 0.875\,\mathrm{Na^{+}} - 0.829\,\mathrm{Cl^{-}} - 0.572\,\mathrm{NO_3^{-}} - 0.834\,\mathrm{SO_4^{2-}}$ | 0.994 |
| 14 | Hardness | $\widehat{\mathrm{Hardness}} = -0.050 + 0.001\,\mathrm{EC} + 2.491\,\mathrm{Ca^{2+}} + 4.124\,\mathrm{Mg^{2+}} - 0.008\,\mathrm{Na^{+}}$ | 1.000 |
| 15 | SAR | $\widehat{\mathrm{SAR}} = 4.073 - 0.012\,\mathrm{Alk} + 0.020\,\mathrm{Na^{+}} - 0.008\,\mathrm{Cl^{-}} - 0.002\,\mathrm{SO_4^{2-}}$ | 0.987 |
| 16 | Boron | $\hat{\mathrm{B}} = -0.297 + 0.005\,\mathrm{Mg^{2+}} - 0.012\,\mathrm{NO_3^{-}} - 0.021\,\mathrm{DO} - 0.001\,\mathrm{EC} + 0.003\,\mathrm{Ca^{2+}} + 0.002\,\mathrm{Na^{+}} - 0.001\,\mathrm{SO_4^{2-}}$ | 0.990 |

$R^2$ values, many of which are nearly equal to 1.00, indicate an excellent level of explanation of variance in the dependent variable, suggesting high predictive re-

liability within the observed dataset. Each equation represents a statistical model describing the joint influence of multiple explanatory variables on the concentration of the target element. To support proper interpretation of the regression coefficients, a representative model is presented below. The same interpretive framework may then be applied to all subsequent models.

**Model 6:** For instance, Equation 6 models Sodium concentrations ($mg{\cdot}L^{-1}$) throughout the year as follows:

$$\widehat{Na^{+}} = -309.576 - 0.66612\,Mg^{2+} + 0.473\,Cl^{-} + 1.851\,NO_3^{-} + 0.250\,SO_4^{2-} + 0.450\,Alk + 22.397\,SAR + 26.282\,B + 2.427\,CB - 0.678\,Ca^{2+},\ with\ R^2 = 0.999.$$

Each regression coefficient represents the expected change in sodium concentration ($Na^{+}$, $mg{\cdot}L^{-1}$) associated with a one-unit increase in the corresponding predictor, while holding all other variables constant. The exceptionally high coefficient of determination ($R^2 = 0.999$) indicates that this multivariate model nearly completely explains the variability in sodium concentrations, underscoring the strong coupling between $Na^{+}$ and the overall ionic, carbonate, and salinity framework of the Zacate Creek.

1) *Regression coefficient of* $Mg^{2+} = -0.666$**:** A 1 $mg{\cdot}L^{-1}$ increase in magnesium results in a 0.666 $mg{\cdot}L^{-1}$ decrease in sodium. This inverse relationship suggests competitive ion exchange processes, where $Mg^{2+}$ displaces $Na^{+}$ from solution through adsorption onto sediments or clay minerals. Divalent cations such as $Mg^{2+}$ have a higher affinity for exchange sites, thereby reducing dissolved sodium under conditions of increasing hardness.

2) *Regression coefficient of* $Cl^{-} = +0.473$**:** An increase of 1 $mg{\cdot}L^{-1}$ in chloride increases $Na^{+}$ by 0.473 $mg{\cdot}L^{-1}$. This positive association reflects the common origin of $Na^{+}$ and $Cl^{-}$ from halite dissolution, evaporative concentration, or anthropogenic inputs such as irrigation return flows. Their coupled behavior is typical of salinity-driven systems and confirms sodium's role as a dominant conservative ion.

3) *Regression coefficient of* $NO_3^{-} = +1.851$: A 1 $mg{\cdot}L^{-1}$ increase in nitrate corresponds to a 1.851 $mg{\cdot}L^{-1}$ increase in sodium. This relationship suggests that nutrient enrichment is accompanied by enhanced sodium loading, likely from agricultural runoff, fertilizer application, or wastewater inputs. Nitrate thus serves as an indicator of anthropogenic influence that simultaneously elevates $Na^{+}$ concentrations.

4) *Regression coefficient of* $SO_4^{2-} = +0.250$**:** Each 1 $mg{\cdot}L^{-1}$ increase in sulfate increases sodium by 0.250 $mg{\cdot}L^{-1}$. This moderate positive effect implies co-mobilization of sulfate and sodium through evaporite dissolution or oxidation of sulfide minerals. Under concentrated flow conditions, sulfate contributes to ionic strength without strongly suppressing $Na^{+}$ availability.

5) *Regression coefficient of Alkalinity* = +0.450: A one-unit increase in alkalinity results in a 0.450 $mg{\cdot}L^{-1}$ increase in sodium. Elevated alkalinity reflects enhanced carbonate weathering and groundwater influence, both of which are commonly associated with sodium-rich waters. This linkage highlights the role of carbonate buffering systems in sustaining dissolved $Na^{+}$ levels.

6) *Regression coefficient of SAR* = +22.397**:** A unit increase in Sodium Adsorption Ratio leads to a substantial 22.397 $mg{\cdot}L^{-1}$ increase in $Na^+$. This strong positive relationship is expected, as SAR directly incorporates sodium concentration relative to calcium and magnesium. High SAR conditions indicate sodium dominance and reduce divalent cation control, reinforcing $Na^+$ accumulation in solution.

7) *Regression coefficient of B* = +26.282: A 1 $mg{\cdot}L^{-1}$ increase in boron increases sodium by 26.282 $mg{\cdot}L^{-1}$, indicating a strong association between these constituents. Boron is commonly enriched in saline groundwater, geothermal inputs, or agricultural return flows, all of which are typically sodium rich. This relationship further supports the influence of deep or anthropogenically modified water sources.

8) *Regression coefficient of CB* = +2.427: An increase of 1% in charge balance increases sodium by 2.427 $mg{\cdot}L^{-1}$. This suggests that $Na^+$ plays a key role in maintaining ionic equilibrium within the system, acting as a compensatory ion when minor charge imbalances occur among measured constituents.

9) *Regression coefficient of* $Ca^{2+}$ = –0.678: A 1 $mg{\cdot}L^{-1}$ increase in calcium results in a 0.678 $mg{\cdot}L^{-1}$ decrease in sodium. This inverse relationship reflects cation exchange and competitive geochemical controls, where increased $Ca^{2+}$ availability suppresses $Na^+$ through adsorption or precipitation-driven processes. It also indicates a transition from sodium-dominated to calcium-dominated water chemistry under higher hardness conditions.

*Overall interpretation*. This sodium model highlights the dominant role of salinity processes, ion exchange, and anthropogenic inputs in controlling $Na^+$ concentrations. Sodium increases with indicators of salinity, nutrient enrichment, alkalinity, and boron, while being suppressed by divalent cations such as calcium and magnesium. The exceptionally high explanatory power of the model suggests that sodium behavior in the system is tightly regulated by integrated hydrogeochemical mechanisms, including evaporative concentration, groundwater mixing, agricultural return flows, and sediment-water ion exchange.

### 4.5. Seasonal Variability and Statistical Significance of Sea-Salt Contributed and Weathered Parameters in Zacate Creek

Separating the chemical concentrations of base cations and sulfate from sea-salt contributions is essential for accurately understanding their release rates from chemical weathering processes [32]. Generally elemental molar ratios in seawater are used to estimate the Sea-Salt derived ions in waters and this approach has been used by various authors in earlier studies from various regions [33]-[36].

To assess the seasonal variability of selected sea salt contributed denoted with (SS) and non-sea salt weathered denoted with asterisk (*) for major base cations and sulfate in Zacate Creek, a one-way Analysis of Variance (ANOVA) was conducted. The objective was to test the null hypothesis that seasonal temperature differences exert no statistically significant influence on these parameters. The results (**Table 5**) revealed distinct and statistically significant seasonal differences (p

< 0.05) in all measured ions, indicating that temperature-driven processes play a critical role in regulating the geochemical behavior of Sea-Salt derived constituents.

**Table 5.** Seasonal variability and statistical significance of Sea-Salt contributed and weathered contributed major base cations and sulfate ions in Zacate Creek.

| Chemical Parameters | Fall Mean ± SD | Winter Mean ± SD | Summer Mean ± SD | F | DF | p-value |
|---|---|---|---|---|---|---|
| SS-$Na^+$ (%) | 49.1 ± 5.7 | 52.7 ± 8.3 | 45.7 ± 6.6 | 2.482 | (2, 27) | 0.102 |
| *$Na^+$ (%) | 50.9 ± 5.8 | 47.3 ± 8.3 | 54.3 ± 6.6 | 2.482 | (2, 27) | 0.102 |
| SS-$Mg^{2+}$ (%) | 45.2 ± 9.2 | 42.4 ± 7.0 | 45.3 ± 9.7 | 0.360 | (2, 27) | 0.701 |
| *$Mg^{2+}$ (%) | 54.8 ± 9.2 | 57.6 ± 7.0 | 54.7 ± 9.7 | 0.360 | (2, 27) | 0.701 |
| SS-$Ca^{2+}$ (%) | 4.6 ± 1.2 | 5.1 ± 1.6 | 4.6 ± 1.6 | 0.433 | (2, 27) | 0.653 |
| *$Ca^{2+}$ (%) | 95.4 ± 1.2 | 94.9 ± 1.6 | 95.4 ± 1.6 | 0.433 | (2, 27) | 0.653 |
| SS- $SO_4^{2-}$ (%) | 6.1 ± 0.7 | 6.4 ± 0.4 | 5.2 ± 1.1 | 6.089 | (2, 27) | 0.007# |
| * $SO_4^{2-}$ (%) | 93.9 ± 0.7 | 93.6 ± 0.4 | 94.8 ± 1.1 | 6.089 | (2, 27) | 0.007# |

Note: SS = Sea-Salt contributed; (*) non-sea-salt (weathered) contributed; # = Statistically significant.

The Sea-Salt (SS) contribution to major ions in Zacate Creek shows distinct patterns among elements and seasons. We present the individual results and interpretations for each ion for Sea-Salt contributed elements as follows.

**1) Sea-Salt derived sodium (SS-$Na^+$):** Sea-Salt-derived sodium (SS-$Na^+$) accounts for approximately half of the total sodium concentration across all seasons, with mean contributions of 49.1% in fall, 52.7% in winter, and 45.7% in summer. Although winter exhibits a slightly higher SS-$Na^+$ contribution, the seasonal differences are not statistically significant ($p = 0.102$), indicating relatively consistent marine or evaporative influence on sodium throughout the year.

**2) Sea-Salt-derived magnesium (SS-$Mg^{2+}$):** Sea-Salt-derived magnesium (SS-$Mg^{2+}$) contributes about 42% - 45% of total magnesium across seasons, with minimal variation among fall, winter, and summer. The lack of significant seasonal difference ($p = 0.701$) suggests that the marine or atmospheric input of magnesium remains stable year-round and is not strongly affected by seasonal hydrological changes in the creek.

**3) Sea-Salt-derived calcium (SS-$Ca^{2+}$):** In contrast, the sea-salt contribution to is very small, averaging only about 4% - 5% in all seasons, and shows no significant seasonal variation ($p = 0.653$). This consistently low SS-$Ca^{2+}$ fraction indicates that calcium in Zacate Creek is overwhelmingly derived from non-marine sources, with negligible influence from sea-salt inputs regardless of season.

**4) Sea-Salt-derived sulfate (SS- $SO_4^{2-}$):** As shown in Figure 4 below, sea-salt-derived sulfate (SS- $SO_4^{2-}$) exhibits a comparatively low but statistically significant seasonal pattern ($p = 0.007$). SS- $SO_4^{2-}$ contributions are highest in winter (6.4%), slightly lower in fall (6.1%), and lowest in summer (5.2%). This seasonal decline suggests that marine or atmospheric sulfate inputs are relatively more important

during cooler, higher-flow conditions, while summer conditions enhance dilution or increase the relative dominance of non-sea-salt sulfate sources in Zacate Creek.

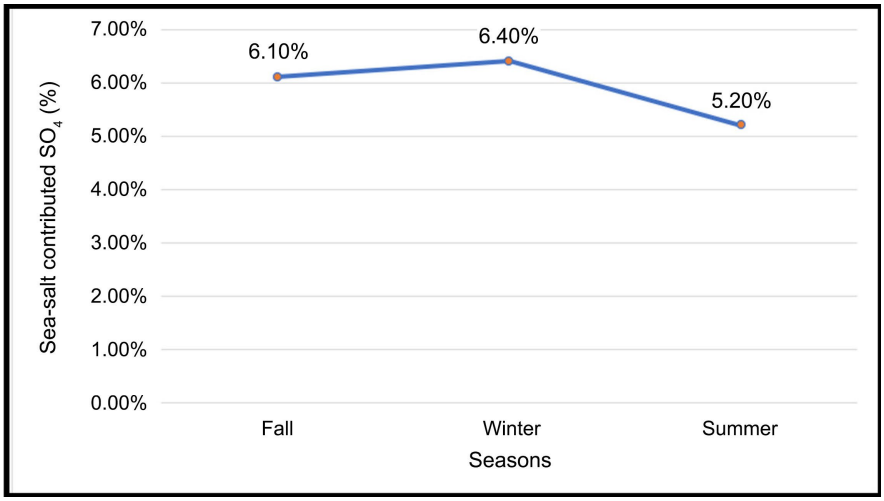


**Figure 4.** Sea-Salt-derived sulfate (SS- $SO_4^{2-}$ ).

## Relative Contributions of Sea-Salt and Weathering-Derived Magnesium across Zacate Creek Samples

**Figure 5** below illustrates the relative contributions of Sea-Salt derived magnesium (SS-$Mg^{2+}$) and non-sea-salt magnesium (*$Mg^{2+}$) across ten Zacate Creek samples (ZCS 1 to ZCS 10). Each stacked bar represents the total magnesium contribution (100%), partitioned into SS-$Mg^{2+}$ (lower, blue segment) and *$Mg^{2+}$ (upper, orange segment), allowing direct comparison of source dominance among samples.

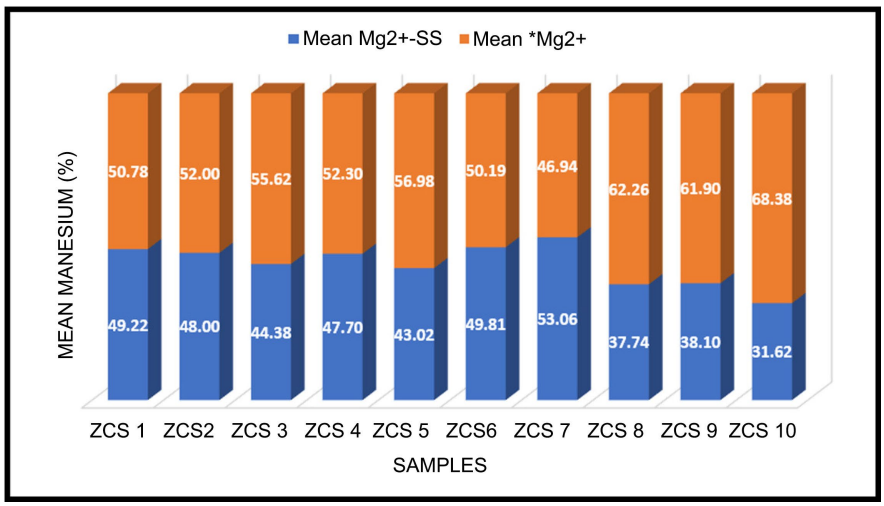


**Figure 5.** Relative contribution of sea salt contributed and non-sea salt (weathered) magnesium to the total magnesium in percentage in Zacate Creek in Laredo, Texas. SS-$Mg^{2+}$ and *$Mg^{2+}$ represent sea-salt and non-sea salt (weathering) contributed magnesium, respectively.

Across ZCS 1 to ZCS 6, SS-$Mg^{2+}$ and *$Mg^{2+}$ contribute nearly equally, with each

accounting for roughly 43% - 50% of total magnesium. This near balance suggests mixed marine/atmospheric and weathering-related sources of magnesium in these samples. ZCS 7 shows a slight shift toward SS-$Mg^{2+}$ dominance (≈53%), indicating a relatively stronger sea-salt or evaporative influence at that site.

In contrast, samples ZCS 8 to ZCS 10 display a pronounced dominance of *$Mg^{2+}$, with non-sea-salt contributions increasing substantially from about 62% in ZCS 8 and ZCS 9 to nearly 68% in ZCS 10. Correspondingly, SS-$Mg^{2+}$ declines to its lowest values (approximately 32% - 38%) in these samples. This trend indicates increasing influence of non-marine sources, most likely enhanced rock weathering, groundwater interaction, or localized geochemical processes contributing magnesium downstream or under changing hydrological conditions (high discharge in lower transects of the Zacate Creek) as downstream site receives urban drainage inputs from various points, so we observed relatively higher discharge than the headwater sites.

Overall, the figure highlights a clear spatial shift from relatively balanced magnesium sources in earlier samples toward strong non-sea-salt dominance in later samples, emphasizing heterogeneity in magnesium origin within Zacate Creek and suggesting increasing importance of catchment-derived weathering inputs relative to marine or atmospheric contributions.

## 5. Discussion

The seasonal ANOVA and Bonferroni post hoc results indicate that water chemistry in Zacate Creek is largely stable across seasons, with notable exceptions driven primarily by winter-summer contrasts. The significantly higher winter concentrations of $Mg^{2+}$, $HCO_3^-$, hardness, and alkalinity suggest increased contributions from carbonate weathering and groundwater inputs, potentially amplified by reduced dilution during lower winter streamflow. Similarly, the pronounced winter peaks in nitrate point to seasonally elevated nutrient loading or diminished biological uptake during colder months, when primary productivity is reduced. The stream flow was too low during summer, and the temperature was too high compared to winter and hence residence time of water might be high and as a consequence nutrients such as nitrate and potassium (K) uptake rates by microbial activities and vegetation along the drainage network were high and consequently potassium and nitrate concentration appeared too low during summer months and high in winter months. The rise in temperature particularly during summer months leads to elevated Gross Primary Productivity (GPP) and hence rapid nitrate and potassium uptake, as nitrate utilization scales with productivity and variation of nitrate as a function of GPP in various aquatic ecosystems has already been documented in different aquatic ecosystems [25] [37].

In contrast, summer conditions are characterized by comparatively lower ionic strength and nutrient concentrations, likely reflecting increased dilution from precipitation events and enhanced biological assimilation during high temperatures. The average monthly precipitation for our sampling period was 12.7 mm,

34.80 mm, and 71.63 mm respectively for the fall (September), winter (Early March) and summer (May) months [29]. Precipitation clearly shows variation in discharge, which ultimately affects the chemical concentration. The lack of significant seasonal variation in parameters such as EC, TDS, $Na^+$, and $Cl^-$ further suggests that the dominant sources of dissolved salts remain relatively constant throughout the year. Overall, these findings highlight winter as a critical period for elevated solute and nutrient concentrations while nutrient depletion occurs during summer months in Zacate Creek, with important implications for understanding seasonal hydrogeochemical controls and potential water quality management considerations.

The bivariate analysis highlights a tightly coupled hydrochemical system in Zacate Creek, where electrical conductivity and total dissolved solids exhibit exceptionally strong correlations with major ions, hardness, SAR, and boron. The consistently high correlation coefficients ($|r| \geq 0.85$) and coefficients of determination ($R^2$ often exceeding 0.90) obviously indicate that variations in EC and TDS are primarily governed by dissolved ionic loads, reflecting shared geochemical sources and transport processes. Figure 6 shows a strong positive linear relationship between the combined non-sea-salt calcium and magnesium ($*Ca^{2+} + *Mg^{2+}$) and non-sea-salt sulfate ($*SO_4^{2-}$) concentrations in Zacate Creek. The fitted regression ($*Ca + *Mg = 0.420 \cdot *SO_4 + 3.718$) explains a large proportion of the variance ($R^2 = 0.851$; $p < 0.001$), indicating that increases in sulfate are closely accompanied by increases in weathering-derived Ca and Mg. This tight coupling suggests a common geochemical control, likely the pyrite oxidation coupled with carbonate dissolution within the creek, with limited influence from independent or external sulfate sources.

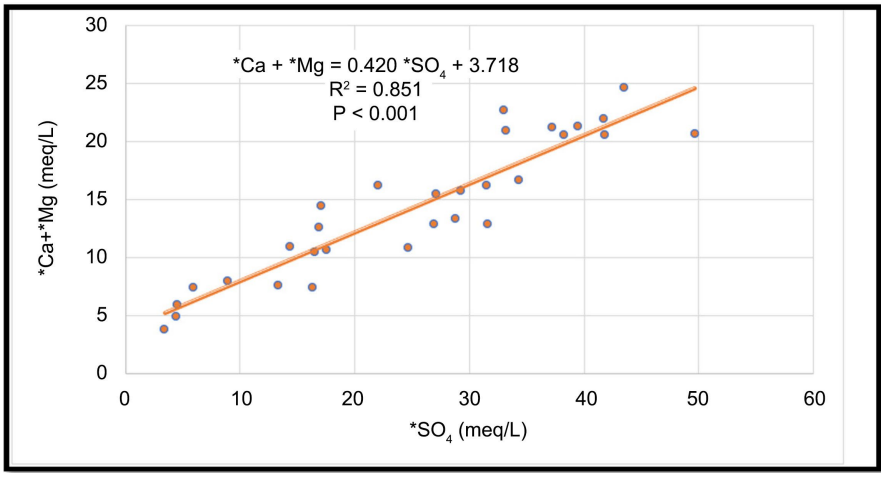


Figure 6. Bivariate relationship between non-sea-salt sum of calcium and magnesium (*Ca + *Mg) and sulfate ($*SO_4$) in Zacate Creek water.

Strong interrelationships among sodium, chloride, sulfate, hardness, and SAR suggest common controls such as mineral dissolution, evaporative concentration, and groundwater contributions, rather than isolated or episodic inputs. The nearly

perfect relationship between bicarbonate and alkalinity further confirms carbonate buffering as a key process regulating the creek's acid-base chemistry and we assume dominant fraction of bicarbonate in alkalinity. Collectively, these results demonstrate that the hydrochemistry of Zacate Creek is dominated by integrated ionic processes, where changes in one parameter reliably reflect concurrent changes in others, underscoring the suitability of EC and TDS as robust integrative indicators of overall water quality and salinity dynamics in the system.

The spatial-temporal multivariate models demonstrate that the hydrochemical behavior of Zacate Creek is highly structured and internally consistent, with water quality parameters responding to tightly coupled geochemical controls that vary modestly by season. The separation of season-specific models for parameters exhibiting significant seasonal variation, alongside unified annual models for seasonally stable parameters, provides a nuanced representation of both temporal dynamics and system-wide interactions. The consistently high $R^2$ values indicate that variability in key constituents is largely explained by interactions among major ions, carbonate species, salinity indicators, and charge balance relationships, underscoring the deterministic nature of the system within the observed dataset. In particular, the sodium model illustrates how $Na^+$ concentrations are amplified by salinity-related variables ($Cl^-$, $SO_4^{2-}$, SAR, boron, alkalinity) and suppressed by divalent cations ($Ca^{2+}$ and $Mg^{2+}$), reflecting the combined influence of evaporative concentration, ion exchange, groundwater mixing, and anthropogenic inputs such as urban runoff and agricultural return flows. Seasonal models for magnesium, nitrate, bicarbonate, alkalinity, and hardness further indicate that winter conditions enhance ionic strength and carbonate influence, whereas summer chemistry reflects dilution and biological moderation. Overall, these multivariate results highlight a highly interconnected hydrogeochemical framework in which changes in individual parameters propagate predictably across the system, reinforcing the value of multivariate modeling for interpreting complex surface-water chemistry and informing water quality management in Zacate Creek.

Partitioning major ions into Sea-Salt derived and non-sea-salt (weathering derived) components provides critical insight into the dominant geochemical processes regulating Zacate Creek water chemistry. The results indicate that sodium and magnesium receive substantial and relatively stable sea-salt contributions across seasons, suggesting persistent atmospheric, evaporative, or recycled saline inputs that are largely insensitive to seasonal hydrologic variability. In contrast, calcium is overwhelmingly derived from non-marine sources throughout the year, confirming carbonate and silicate weathering as its primary control. Notably, Sea-Salt derived sulfate exhibits statistically significant seasonal variation, with higher contributions during winter and lower contributions in summer, reflecting enhanced atmospheric deposition or reduced dilution under cooler, higher-flow conditions, followed by increased dominance of non-sea-salt sulfate during warmer periods. Spatial patterns in magnesium further reveal a downstream shift from mixed marine and weathering sources toward strong weathering dominance, in-

dicating increasing groundwater interaction or enhanced mineral dissolution along the flow path. Collectively, these findings demonstrate that while sea-salt inputs provide a consistent background signal for certain ions, seasonal hydrology and catchment scale weathering processes exert a stronger and more variable influence on sulfate and magnesium dynamics, underscoring the importance of source apportionment in interpreting surface water geochemistry in semi-arid environments such as Zacate Creek.

## 6. Conclusion

Water samples from Zacate Creek, a small urban tributary to Rio Grande in Laredo, southern Texas, were analyzed to evaluate the factors controlling water quality parameters and their spatiotemporal trends along the drainage network. The major cations and anions existed in the order $Na^+ \gg Ca^{2+} > Mg^{2+} \approx K^+$ and $SO_4^{2-} \gg Cl^- > HCO_3^- \gg NO_3^- \gg PO_4^{3-}$, respectively. Natural chemical weathering contributed to the solute load, but marine aerosols (sea-salt inputs) accounted for approximately 44% of total magnesium and 49% of total sodium concentrations. In contrast, calcium and sulfate showed higher contributions from chemical weathering processes. Potassium appeared negligible from weathering because of rapid uptake by microbes and vegetation during summer months. The elevated Gross Primary Productivity (GPP) is expected during summer months due to rapid nitrate and potassium uptake, as nitrate utilization scales with productivity due to high photosynthetic and microbial growth rates with high temperature during summer months. Calcite and siliciclastic weathering appear to be the dominant geochemical controls followed by sea-salt contribution to water chemistry along the Zacate Creek. Anthropogenic inputs, particularly urban runoff, and dry atmospheric deposition, also contribute measurable chemical loads to the system. Winter concentrations of $Mg^{2+}$, $HCO_3^-$, hardness, and alkalinity appeared significantly higher due to enhanced carbonate weathering and groundwater inputs, potentially amplified by reduced dilution. Sea-Salt derived sulfate exhibits statistically significant seasonal variation, with higher contributions during winter and lower contributions in summer, reflecting enhanced atmospheric deposition due to climatic conditions or reduced dilution under cooler, higher-flow conditions. Sodium adsorption ratios (SAR = 8.5), suggesting water is not suitable for all types of vegetation in the long run. Overall water quality is suitable for most uses including irrigation for most of the crops except for high salt content.

## Acknowledgements

The authors would like to thank Aaron Sanchez at the Center for Earth and Environmental Studies of Texas A & M International University for his help in producing the sampling area map (**Figure 1**). The authors acknowledge the Welch Foundation Grant No. BS-0051 for supporting this research. The authors wish to thank the members of the editorial office for their efficient management of this submission. Authors are also grateful to the editors and anonymous reviewers for

their constructive feedback and insightful comments, which have significantly improved the overall strength of this paper.

## Authors' Contributions

MPB designed, implemented, and supervised the project, conducted the chemistry data analysis, and led the manuscript writing, reviewing, and editing; PK and ET carried out field sampling, participated in writing and reviewing; SB assisted with chemistry data processing and participated in writing and reviewing. GBM performed data analysis using multivariate modeling and contributed to writing, reviewing, and editing. AAM contributed to methodology development, funding acquisition, writing, reviewing, and editing.

## Conflicts of Interest

The authors declare no conflicts of interest.

## References

[1] Scanlon, B.R., Keese, K.E., Flint, A.L., Flint, L.E., Gaye, C.B., Edmunds, W.M., *et al.* (2006) Global Synthesis of Groundwater Recharge in Semiarid and Arid Regions. *Hydrological Processes*, **20**, 3335-3370. https://doi.org/10.1002/hyp.6335

[2] Vörösmarty, C.J., McIntyre, P.B., Gessner, M.O., Dudgeon, D., Prusevich, A., Green, P., *et al.* (2010) Global Threats to Human Water Security and River Biodiversity. *Nature*, **467**, 555-561. https://doi.org/10.1038/nature09440

[3] IPCC (2021) Climate Change 2021: The Phyiscal Science Basis. Contribution of Working Group I to the Sixth Assessment Report of the Intergovernmental Panel on Clime Change. Cambridge University Press, 2391 p.

[4] UN Water and WMO (2021) Climate Change, Population Increase Fuel Looming Water Crisis. United Nations-World Meteorological Organization, Global Perspective Human Stories. https://news.un.org/en/story/2021/10/1102162

[5] UNESCO (2025) The United Nations World Water Development Report 2025, Mountains and Glaciers: Water Towers. UNESCO World Water Assessment Programme. p. 174.

[6] Gunnarsdottir, M.J., Gardarsson, S.M., Jonsson, G.S. and Bartram, J. (2016) Chemical Quality and Regulatory Compliance of Drinking Water in Iceland. *International Journal of Hygiene and Environmental Health*, **219**, 724-733. https://doi.org/10.1016/j.ijheh.2016.09.011

[7] Bhatt, M.P., Malla, G.B. and McDowell, W.H. (2024) Comprehensive Assessment and Analysis of Drinking Water Quality in the Kathmandu Valley: Implications for Public Health and Policy. *American Journal of Water Resources*, **12**, 149-164. https://doi.org/10.12691/ajwr-12-4-5

[8] Datry, T., Larned, S.T. and Tockner, K. (2014) Intermittent Rivers: A Challenge for Freshwater Ecology. *BioScience*, **64**, 229-235. https://doi.org/10.1093/biosci/bit027

[9] Costigan, K.H., Jaeger, K.L., Goss, C.W., Fritz, K.M. and Goebel, P.C. (2016) Understanding Controls on Flow Permanence in Intermittent Rivers to Aid Ecological Research: Integrating Meteorology, Geology and Land Cover. *Ecohydrology*, **9**, 1141-1153. https://doi.org/10.1002/eco.1712

[10] Regier, P.J., González-Pinzón, R., Van Horn, D.J., Reale, J.K., Nichols, J. and

Khandewal, A. (2020) Water Quality Impacts of Urban and Non-Urban Arid-Land Runoff on the Rio Grande. *Science of The Total Environment*, **729**, Article 138443. https://doi.org/10.1016/j.scitotenv.2020.138443

[11] Wang, X., Tang, J., Liu, G., Zhu, M., Wan, Q., Li, B., *et al.* (2025) Hydrological-Geochemical Controls on Seasonal Rare Earth Element Dynamics in Semi-Arid Mining Riparian Zones: Implications for Sustainable Remediation. *Journal of Environmental Chemical Engineering*, **13**, Article 120051. https://doi.org/10.1016/j.jece.2025.120051

[12] McClain, M.E., Boyer, E.W., Dent, C.L., Gergel, S.E., Grimm, N.B., Groffman, P.M., *et al.* (2003) Biogeochemical Hot Spots and Hot Moments at the Interface of Terrestrial and Aquatic Ecosystems. *Ecosystems*, **6**, 301-312. https://doi.org/10.1007/s10021-003-0161-9

[13] Zimmer, M.A., Burgin, A.J., Kaiser, K. and Hosen, J. (2022) The Unknown Biogeochemical Impacts of Drying Rivers and Streams. *Nature Communications*, **13**, Article No. 7213. https://doi.org/10.1038/s41467-022-34903-4

[14] Baeza, M., Ren, J., Krishnamurthy, S. and Vaughan, T.C. (2009) Spatial Distribution of Antimony and Arsenic Levels in Manadas Creek, an Urban Tributary of the Rio Grande in Laredo, Texas. *Archives of Environmental Contamination and Toxicology*, **58**, 299-314. https://doi.org/10.1007/s00244-009-9357-0

[15] Tao, Z., Huang, M., Jia, X. and Wang, H. (2025) Topography-Driven Hydrochemical Evolution in Semi-Arid Watershed: Isotopic and Seasonal Insights into Surface Water-Groundwater Interactions. *Journal of Hydrology*: *Regional Studies*, **62**, Article 102940. https://doi.org/10.1016/j.ejrh.2025.102940

[16] Gibbs, R.J. (1970) Mechanisms Controlling World Water Chemistry. *Science*, **170**, 1088-1090. https://doi.org/10.1126/science.170.3962.1088

[17] Stallard, R.F. and Edmond, J.M. (1983) Geochemistry of the Amazon: 2. The Influence of Geology and Weathering Environment on the Dissolved Load. *Journal of Geophysical Research*: *Oceans*, **88**, 9671-9688. https://doi.org/10.1029/jc088ic14p09671

[18] Kaushal, S., McDowell, W., Wollheim, W., Johnson, T., Mayer, P., Belt, K., *et al.* (2015) Urban Evolution: The Role of Water. *Water*, **7**, 4063-4087. https://doi.org/10.3390/w7084063

[19] Kaushal, S.S., Likens, G.E., Pace, M.L., Reimer, J.E., Maas, C.M., Galella, J.G., *et al.* (2021) Freshwater Salinization Syndrome: From Emerging Global Problem to Managing Risks. *Biogeochemistry*, **154**, 255-292. https://doi.org/10.1007/s10533-021-00784-w

[20] Shattuck, M.D., Fazekas, H.M., Wymore, A.S., Cox, A. and McDowell, W.H. (2023) Salinization of Stream Water and Groundwater at Daily to Decadal Scales in a Temperate Climate. *Limnology and Oceanography Letters*, **8**, 131-140. https://doi.org/10.1002/lol2.10306

[21] Creed, I.F., Lane, C.R., Serran, J.N., Alexander, L.C. Basu, N.B., *et al.* (2017) The Role of Intermittent Rivers and Ephemeral Streams in Aquatic Ecosystems. *Freshwater Biology*, **62**, 1-19.

[22] Palmer, M.A., Hondula, K.L. and Koch, B.J. (2014) Ecological Restoration of Streams and Rivers: Shifting Strategies and Shifting Goals. *Annual Review of Ecology*, *Evolution*, *and Systematics*, **45**, 247-269. https://doi.org/10.1146/annurev-ecolsys-120213-091935

[23] Bhatt, M.P., Rubio, A., Malla, G.B., Lopez, C., Morales, V., Cano, E.V., *et al.* (2024) Evaluation of Human Impacts on Bartlett Pond Ecosystem, Laredo, Southern Texas, USA, through Empirical Modeling. *Journal of Environmental Protection*, **15**, 497-526. https://doi.org/10.4236/jep.2024.154029

[24] Bhatt, M.P., Malla, G.B., Rubio, A. and Addo-Mensah, A. (2025) Sediment Quality Assessment on Bartlett Pond in Laredo, Southern Texas, USA. *Open Journal of Soil Science*, **15**, 43-69. https://doi.org/10.4236/ojss.2025.151003

[25] Bhatt, M.P., Malla, G.B., Nuño, D.E., Bhatt, S. and Addo-Mensah, A. (2025) Spatio-temporal Variations of Chemical Compositions through Empirical Modeling in Bartlett Pond, Laredo, Texas. *Journal of Water Resource and Protection*, **17**, 976-1003. https://doi.org/10.4236/jwarp.2025.1712051

[26] Animalia (2025) River Rio Grande. Animalia. https://animalia.bio/rio-grande

[27] Rio Grande (2026) American Rivers. https://www.americanrivers.org/river/rio-grande/

[28] Schmandt, J. (2002) Bi-national Water Issues in the Rio Grande/Río Bravo Basin. *Water Policy*, **4**, 137-155. https://doi.org/10.1016/s1366-7017(02)00007-7

[29] US Climate (2025) Climate Data of Laredo. https://www.usclimatedata.com/climate/laredo/texas/united-states/utstx0737

[30] United States Environmental Protection Agency (1991) Methods for Determination of Metals in Environmental Samples. EPA/600/4-91/010, Office of Research and Development.

[31] APHA (1989) Standard Methods for the Examination of Water and Wastewater. American Public Health Association.

[32] Bhatt, M.P., Malla, G.B. and Yde, J.C. (2025) Status and Progress of Determining the Variability and Controls on Chemical Denudation Rates in Glacierized Basins around the World. *Water*, **17**, Article 2811. https://doi.org/10.3390/w17192811

[33] McDowell, W.H., Sánchez, C.G., Asbury, C.E. and Ramos Pérez, C.R. (1990) Influence of Sea Salt Aerosols and Long Range Transport on Precipitation Chemistry at El Verde, Puerto Rico. *Atmospheric Environment. Part A. General Topics*, **24**, 2813-2821. https://doi.org/10.1016/0960-1686(90)90168-m

[34] Millot, R., Gaillardet, J., Dupré, B. and Allègre, C.J. (2002) The Global Control of Silicate Weathering Rates and the Coupling with Physical Erosion: New Insights from Rivers of the Canadian Shield. *Earth and Planetary Science Letters*, **196**, 83-98. https://doi.org/10.1016/s0012-821x(01)00599-4

[35] Bhatt, M.P. and McDowell, W.H. (2007) Controls on Major Solutes within the Drainage Network of a Rapidly Weathering Tropical Watershed. *Water Resources Research*, **43**, W11402. https://doi.org/10.1029/2007wr005915

[36] Bhatt, M.P., Hartmann, J. and Acevedo, M.F. (2018) Seasonal Variations of Biogeochemical Matter Export along the Langtang-Narayani River System in Central Himalaya. *Geochimica et Cosmochimica Acta*, **238**, 208-234. https://doi.org/10.1016/j.gca.2018.06.033

[37] Bernhardt, E.S., Heffernan, J.B., Grimm, N.B., Stanley, E.H., Harvey, J.W., Arroita, M., *et al.* (2017) The Metabolic Regimes of Flowing Waters. *Limnology and Oceanography*, **63**, S99-S118. https://doi.org/10.1002/lno.10726